arXiv:1402.4709v1 [hep-ex] 19 Feb 2014

Comparing pion production models to MiniBooNE data

P. A. Rodrigues

Department of Physics and Astronomy, University of Rochester, Rochester, NY, USA

Abstract. Predictions for neutrino-induced charged- and neutral-current single pion production on CH_2 from theoretical models and Monte Carlo event generators are compared with the cross section measurements from the MiniBooNE experiment.

Keywords: neutrino, cross sections, pion production, resonant, coherent
PACS: 13.15.+g,14.60.Lm,21.60.Ka,25.30.-c

Improved understanding of neutrino-induced single pion production in interactions on nuclei in the $E_\nu \lesssim 1\,\text{GeV}$ region is important for current and upcoming neutrino oscillation experiments, as these processes form backgrounds to both $\nu_\mu \to \nu_e$ appearance and $\nu_\mu \to \nu_\mu$ disappearance signals. Single pion production on nuclei is also interesting in its own right, as it probes features such as the contribution of nonresonant background terms; possible multinucleon contributions to the cross section; and the effect of final state interactions on both the total cross section and differential cross sections in pion kinematic variables.

A key component in answering these questions, and reducing systematic uncertainties for oscillation experiments, is detailed measurement of pion production cross sections on nuclei in a range of channels. The cross section for pion production on individual nucleons was measured in deuterium bubble chambers at ANL [1] and BNL [2] for E_ν around 1 GeV, but these measurements disagree with one another at the 30–40% level, and both have large uncertainties. More recent measurements, taken on plastic scintillator and water, have been made by the K2K [3, 4, 5] experiment, although these are not presented as absolute cross sections.

At NuInt09, a detailed set of comparisons was made between the predictions of a wide range of models for charged current single pion production on carbon [6]. The present study considers a smaller number of models, but includes comparisons to MiniBooNE data which were not available at the time of NuInt09.

MINIBOONE DATA

The most detailed measurements to date of single pion production on nuclei have been made by the MiniBooNE experiment, which produced high-statistics absolute cross sections for charged current single π^+ (CC1π^+) [7], charged current single π^0 (CC1π^0) [8], and neutral current single π^0 (NC1π^0) production [9]. For each of these measurements, a range of differential cross sections in relevant kinematic quantities has been provided, facilitating thorough comparison with model predictions. In each case the signal is defined by the particles exiting the nucleus, rather than particles produced at the interaction vertex, so the results are able to test the combination of nucleon-level cross section, nuclear effects, and final state interactions.

The MiniBooNE data are taken in the Booster neutrino beam, which consists mostly of muon neutrinos, and has a peak neutrino energy of around 600 MeV. The neutrino flux is small beyond about 2 GeV [10]. Differential cross sections provided by MiniBooNE are averaged over this flux.

The three datasets published by MiniBooNE are summarized below:

CC1π^+ The signal is defined as a muon and exactly one π^+ exiting the nucleus, with no other mesons, but any number of nucleons. Resonant and coherent π^+ production can contribute to this sample.

CC1π^0 The signal is defined as a muon and exactly one π^0 exiting the nucleus, with no other mesons, but any number of nucleons. Resonant π^0 production contributes to this sample, along with a potentially significant fraction of resonant π^+ events in which the π^+ charge exchanges in the nucleus. For this sample, MiniBooNE present differential distributions averaged over the neutrino flux from 0.5 to 2 GeV.

NC1π^0 The signal is defined as no muon and exactly one π^0 exiting the nucleus, with no other mesons, but any number of nucleons. Resonant and coherent π^0 production are expected to be the main contributions to this

sample. Measurements have also been made in the $\bar{\nu}_\mu$ flux, but are not considered here.

MODELS USED

The models compared in this work can be broadly divided into two categories, namely theoretical models, and full Monte Carlo (MC) generators. While the theoretical models produce total or differential cross sections for a given process as output, generators produce samples of events suitable for use as input to a full experimental simulation. Predictions for each of the models were kindly provided by the relevant groups.

The theoretical models considered are:

Athar *et al.* This model uses a Δ-dominance assumption with a local density approximation for the nuclear effects. In-medium modifications to the Δ properties are included, along with an MC cascade model of final state effects [11, 12].

GiBUU The GiBUU code provides a unified treatment of nuclear transport processes for interactions of nucleons, nuclei, pions, electrons and neutrinos with nuclei. The code provides a careful treatment of particle transport through the nucleus via the BUU equation. The neutrino-nucleon cross sections for single pion production account for 13 resonances with vector couplings taken from the MAID model for pion photo- and electroproduction, and axial couplings from PCAC. Nonresonant background terms are also included [13].

Nieves *et al.* The model of Nieves *et al.* describes both quasielastic and single pion production processes in the region around 1 GeV. The single pion production description is based on the SU(2) nonlinear σ model, with nonresonant background terms included, and only the Δ resonance considered. The parameters $C_5^A(0)$ and M_A^Δ are tuned to ANL and BNL data, while the nuclear effects are taken from photon, electron and pion interactions with nuclei [14].

The Monte Carlo generators considered are:

GENIE 2.6.2 The Rein-Sehgal model is used for values of the hadronic invariant mass $W < 1.7\,\text{GeV}$, with 16 resonances included. Nuclear effects are treated using the relativistic Fermi Gas model [15].

NEUT 5.1.4.2 NEUT also uses the Rein-Sehgal model, for $W < 2\,\text{GeV}$, along with the relativistic Fermi Gas model. The full set of 18 resonances included used in the Rein-Sehgal paper is included [16].

NuWro NuWro explicitly considers only the Δ resonance, with heavier resonances treated using quark-hadron duality from the DIS cross section. The spectral function is employed for nuclear effects [17].

All three MC generators use their own cascade model for final state effects.

At the time of writing, not all of the models had produced predictions for all of the distributions. Each figure shows all the distributions that were available.

COMPARISONS

Figure 1 shows the total cross sections as a function of energy for CC1π^+ and CC1π^0. The predictions generally fall below the data in the case of CC1π^+, with GENIE coming closest. In CC1π^0, the agreement with data is, on the whole, better, although there is still some tendency for predictions to fall below the data points.

Figure 2 shows the ratio of total cross section prediction to data as a function of energy, for the two CC samples. A few features stand out. Firstly, although the predictions differ significantly in the overall normalization of the cross section, the shapes of the prediction/data ratios, particularly in CC1π^+, are quite similar, being higher at low energies than at higher energies. Secondly, although the CC1π^0 ratios also show similarities between the predictions, the shapes are quite different from the CC1π^+ shapes. This suggests that the discrepancies between the predictions and the MiniBooNE data cannot be solely due to a mismodelling of the flux shape, which would lead to similar shapes in the two cases.

The ability to draw conclusions such as these is one of the advantages of taking the three MiniBooNE pion production data sets together. Less optimistically, the difficulty of obtaining simultaneous agreement with the two CC samples highlights a potential problem for other experiments (especially neutrino oscillation experiments) in using the MiniBooNE data to constrain cross section predictions. An example of this is the T2K oscillation analysis, which introduced *ad hoc* tuning parameters with large uncertainties to reflect the difficulty of obtaining simultaneous agreement with the three MiniBooNE data sets [18].

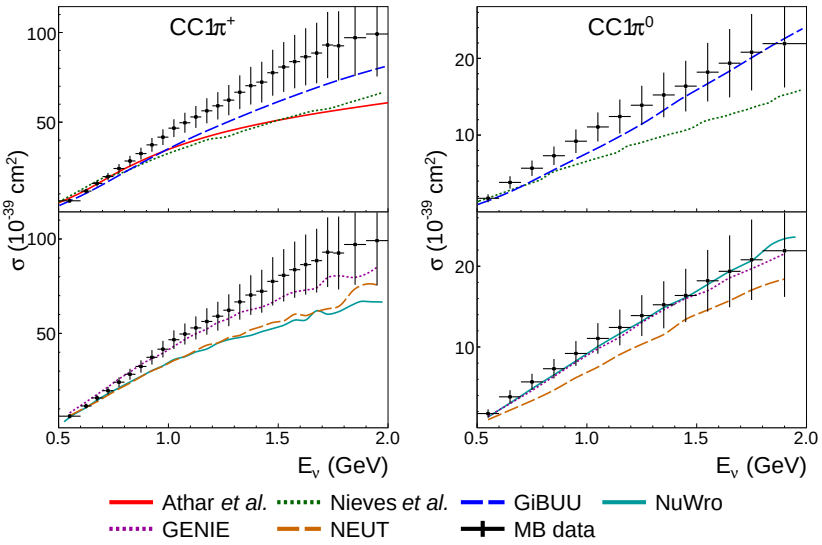

FIGURE 1. CC1π^+ (left) and CC1π^0 (right) total cross sections as a function of neutrino energy for each of the models and for the MiniBooNE data. The top row shows the theoretical model predictions, while the bottom row shows the MC generator predictions. (The data is the same top and bottom.)

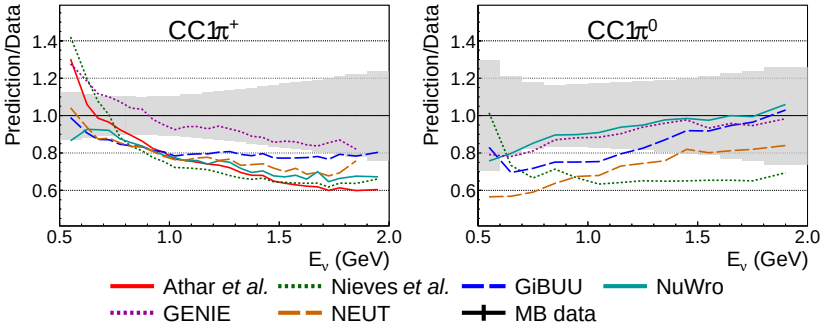

FIGURE 2. Ratios of prediction to MiniBooNE data in the total cross section as a function of energy for CC1π^+ (left) and CC1π^0 (right). The grey shaded region shows the size of the data uncertainty.

Predictions and MiniBooNE data for the differential cross section $d\sigma/dQ^2$, along with ratios, are shown in Figure 3. Again, the predictions differ in overall normalization of the cross section by up to 50%, but show similarities in shape, with the MiniBooNE data having greater strength in the $Q^2 \approx 0.5\,\mathrm{GeV}^2$ region. The differential cross section in muon kinetic energy, shown in Figure 4, is strongly correlated with Q^2, and so shows some differences in the level of agreement, as compared with the $d\sigma/dQ^2$ differential cross section. This suggests some further disagreement in the muon angle distribution.

Figure 5 shows the differential cross sections in pion momentum (kinetic energy for CC1π^+). These distributions are expected to be significantly altered by pion reinteractions within the nucleus, and so potentially provide an important test of final state effects.

There are significant differences in both shape and normalization between the predictions, and a corresponding difference in level of agreement with the data. Lalakulich and Mosel [19] have drawn attention to the region of pion kinetic energy around 0.2 GeV (pion momentum $p_\pi \approx 0.3\,\mathrm{GeV}$), where final state effects should reduce the differential cross section through Δ production. Most of the models show a dip in this region for CC1π^+, which does not appear to be present in the data.

Differential cross sections in pion angle for CC1π^0 and NC1π^0 are shown in Figure 6 (pion angle distributions in CC1π^+ are only provided by MiniBooNE in the form of double-differential cross sections over a limited range in

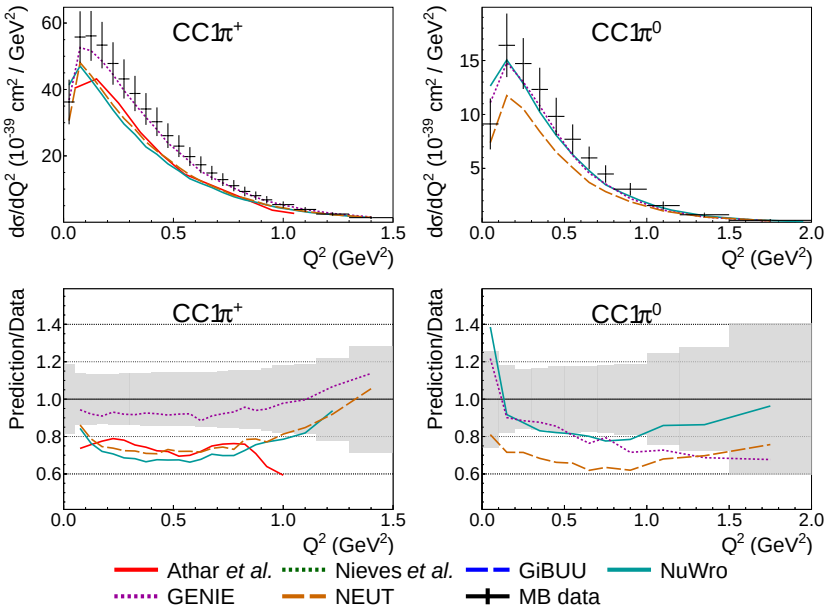

FIGURE 3. Predictions and MiniBooNE data for the flux-averaged differential cross section $\mathrm{d}\sigma/\mathrm{d}Q^2$ for CC1π^+ (left) and CC1π^0 (right). Ratios of the predictions to the MiniBooNE data are shown in the lower row.

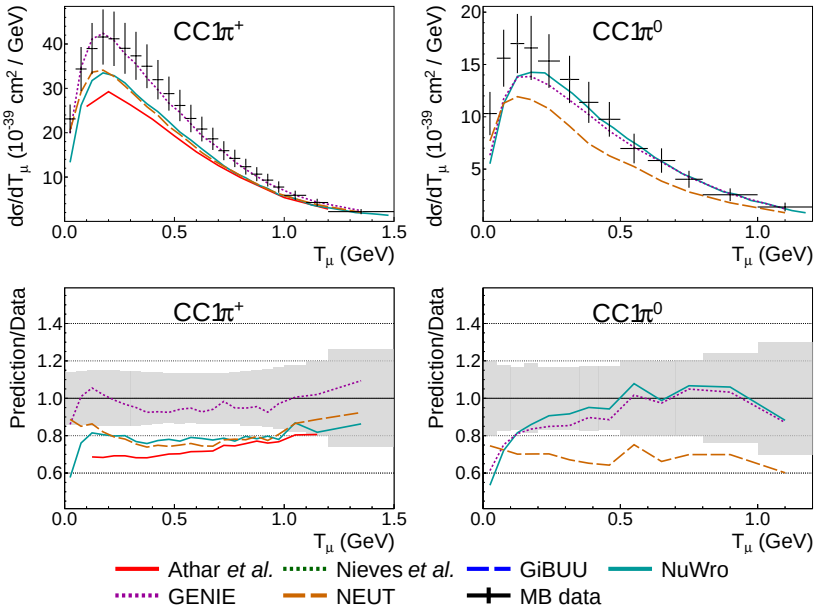

FIGURE 4. Predictions and MiniBooNE data for the flux-averaged differential cross section in muon kinetic energy $\mathrm{d}\sigma/\mathrm{d}T_\mu$ for CC1π^+ (left) and CC1π^0 (right). Ratios of the predictions to the MiniBooNE data are shown in the lower row.

$\cos\theta_\pi$ and are not shown here). While the agreement with data in NC1π^0 is quite good, especially for the generators, the cross section is more forward-peaked in the CC1π^0 data than for all of the predictions.

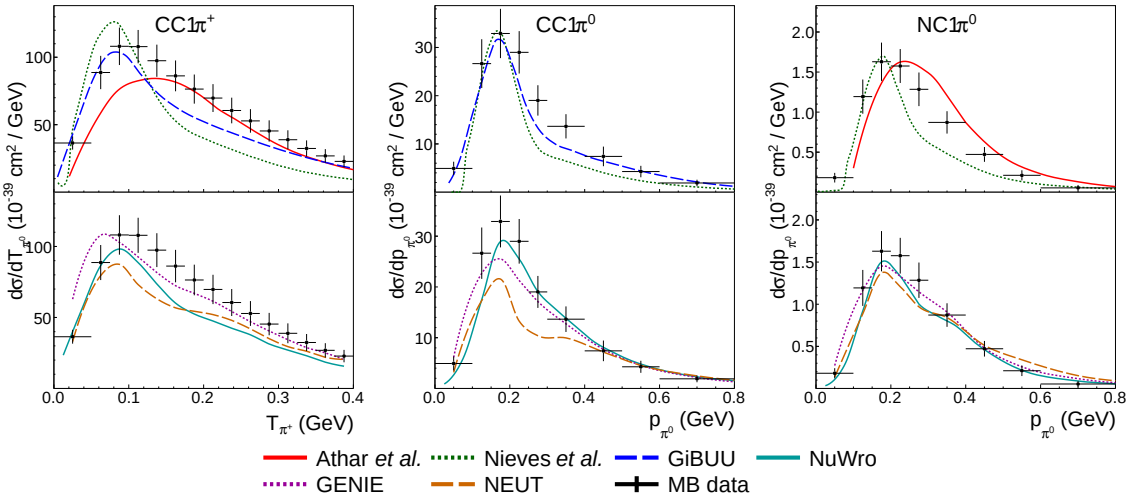

FIGURE 5. Predictions and MiniBooNE data for the differential cross sections in pion kinetic energy for CC1π^+ (left), pion momentum for CC1π^0 (middle), and pion momentum for NC1π^0 (right). The top row shows the theoretical model predictions, while the bottom row shows the MC generator predictions. (The data is the same top and bottom.)

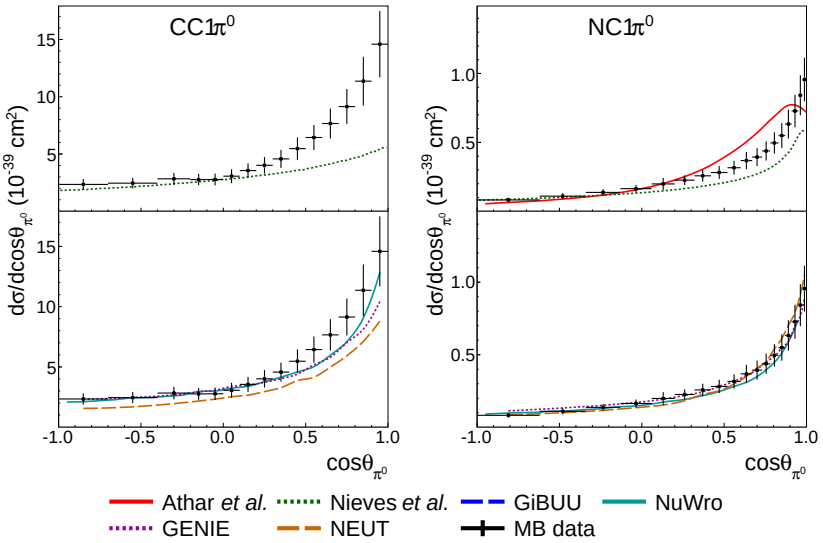

FIGURE 6. Predictions and MiniBooNE data for the differential cross section in pion angle $d\sigma/d\cos\theta_\pi$ for CC1π^0 (left) and NC1π^0 (right). The top row shows the theoretical model predictions, while the bottom row shows the MC generator predictions. (The data is the same top and bottom.)

CONCLUSIONS

Predictions for neutrino-induced pion production from CH_2 have been compared with the data from MiniBooNE. Most models fall below the data in total CC cross section, and there are also some shape disagreements in the differential cross sections. The largest variation between predictions (and, hence, in the level of agreement with data) is in the pion momentum distributions, which suggests differences in final state effects.

The next step in understanding the differences between the predictions will be to compare predictions for neutrino-induced pion production on free nucleons, which are free of nuclear and final state effects.

ACKNOWLEDGEMENTS

Predictions for the models, along with help in understanding the predictions, were kindly provided by M. Athar, S. Chauhan, S. Dytman, H. Gallagher, T. Golan, Y. Hayato, E. Hernandez, O. Lalakulich, U. Mosel, J. Nieves and J. Sobczyk.

REFERENCES

1. G. M. Radecky, et al., *Phys. Rev. D* **25**, 1161–1173 (1982).
2. T. Kitagaki, et al., *Phys. Rev. D* **34**, 2554–2565 (1986).
3. C. Mariani, et al., *Phys. Rev. D* **83**, 054023 (2011).
4. S. Nakayama, et al., *Physics Letters B* **619**, 255 – 262 (2005).
5. A. Rodriguez, et al., *Phys. Rev. D* **78**, 032003 (2008).
6. S. Boyd, S. Dytman, E. Hernández, J. Sobczyk, and R. Tacik, "Comparison of Models of Neutrino-Nucleus Interactions," in *American Institute of Physics Conference Series*, edited by F. Sanchez, M. Sorel, and L. Alvarez-Ruso, 2009, vol. 1189 of *American Institute of Physics Conference Series*, pp. 60–73.
7. A. A. Aguilar-Arevalo, et al., *Phys. Rev. D* **83**, 052007 (2011).
8. A. A. Aguilar-Arevalo, et al., *Phys. Rev. D* **83**, 052009 (2011).
9. A. A. Aguilar-Arevalo, et al., *Phys. Rev. D* **81**, 013005 (2010).
10. A. Aguilar-Arevalo, et al., *Phys.Rev.* **D79**, 072002 (2009).
11. Sajjad Athar, M., Chauhan, S., and Singh, S. K., *Eur. Phys. J. A* **43**, 209–227 (2010).
12. M. Sajjad Athar, S. Chauhan, and S. K. Singh, *Journal of Physics G: Nuclear and Particle Physics* **37**, 015005 (2010).
13. O. Buss, et al., *Phys. Rept.* **512**, 1–124 (2012).
14. J. Nieves, I. Ruiz Simo, and M. Vicente Vacas, *Phys.Rev.* **C83**, 045501 (2011).
15. C. Andreopoulos, et al., *Nucl. Instrum. Meth.* **A614**, 87–104 (2010).
16. Y. Hayato, *Acta Phys. Polon.* **40**, 2477 (2009).
17. T. Golan, C. Juszczak, and J. T. Sobczyk, *Phys. Rev. C* **86**, 015505 (2012).
18. P. A. Rodrigues, "Tuning NEUT-based cross section models for oscillation analysis," in *Proceedings of 14th International Workshop on Neutrino Factories, Super Beams and Beta Beams*, 2013, To appear.
19. O. Lalakulich, and U. Mosel, *Phys.Rev.* **C87**, 014602 (2013).